Step-Driven Lateral Segregation and Long-Range Ordering during Si_xGe_{1-x} Epitaxial Growth

D. E. Jesson and S. J. Pennycook
Solid State Division, Oak Ridge National Laboratory, Oak Ridge, Tennessee 37831-6024

J.-M. Baribeau and D. C. Houghton
Institute for Microstructural Sciences, National Research Council of Canada, Ottawa, Canada K1A 0R6
(Received 27 November 1991)

Lateral segregation occurring at advancing steps is identified as the origin of a new long-range ordered phase in Si_xGe_{1-x} alloys, which has been imaged directly. The segregation occurs at monolayer height type-S_B steps under island growth conditions and is strongly dependent on growth kinetics.

PACS numbers: 68.55.Bd, 68.35.Fx

The growth of Si_xGe_{1-x} alloys by molecular-beam epitaxy (MBE) is of considerable scientific and technological importance, but little is known about the fundamental atomistic processes which govern the surface kinetics and thermodynamics of alloy growth. In this Letter, we identify an important new role of surface steps during the MBE growth of alloy layers. We show that nonequilibrium island growth via nonequivalent steps can produce lateral segregation and long-range ordering without the need for any atomic rearrangements after the completion of the surface layer. Specifically, we explain ordering in the Si-Ge system, although lateral segregation will also occur in the growth of other technologically important ternary alloys such as GaInP and AlGaAs.

Since the initial observation of additional periodicities occurring in Si-Ge alloy layers [1], considerable effort has been directed towards understanding ordering in this system. Recent theoretical and experimental studies have concluded that ordering must be growth induced [2-7]. The final ordered microstructure, therefore, provides a unique fingerprint of the atomistic processes which have occurred during MBE growth. Using the recently developed Z-contrast scanning transmission electron microscopy technique [8], it is now possible to image the ordered microstructure directly, and to deduce important information on the atomic-scale growth processes. Figure 1 represents the first image of ordering in Si-Ge alloys and unambiguously reveals the nature of the ordered phase. Every alternate (111) plane appears bright, and lower magnification images reveal that the ordering is long range in the [001] growth direction with a relatively small lateral domain size (~20 nm). This is a remarkable result demonstrating that significant ordering and phase locking can occur during low-temperature growth at only 350 °C, which is inconsistent with all current alloy growth models [10] and therefore poses fundamental questions regarding the origin of the ordering.

To explain ordering in Si_xGe_{1-x} alloys, we now propose a mechanism which is consistent with the highly nonequilibrium nature of MBE growth. By analogy with Si homoepitaxy, we assume that growth occurs via monolayer height islands and the consecutive interchange of (1×2) and (2×1) domains [11,12]. The islands are strongly anisotropic and, using the notation of Chadi [13], growth occurs mainly via type-S_B steps. At high supersaturations, growth is forced alternately through low- and high-energy type-S_B step configurations in response to the translational symmetry of the (2×1) surface reconstruction. Consider now the important role of this geometry during codeposition of Si and Ge atoms.

Figure 2 shows a schematic representation of rebonded and nonrebonded type-S_B step configurations, together with relevant adatom energy-level diagrams. The shaded binding sites correspond to the deep potential wells just ahead of the growing step edges. Clearly, Ge with its lower surface energy of about 0.1 eV/atom compared with Si [14] will linger longer at both step edges, and is

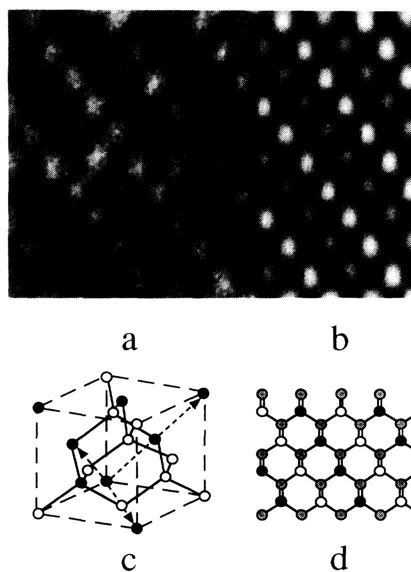

FIG. 1. (a) [110] Z-contrast image of an ordered $Si_{0.6}Ge_{0.4}$ alloy deposited at 0.24 nm s^{-1} on a Si(001) substrate at 350±25 °C [9]. The accompanying simulation (b) is generated from the [110] projection (d) of the ordered phase (c) predicted by our lateral segregation model. Each bright spot in the image corresponds to a [110] atomic dumbbell, and the column intensities approach the atomic-number-squared dependence of unscreened Rutherford scattering. The open, solid, and shaded circles represent Ge-rich, Si-rich, and deposited alloy compositions, respectively. In (c) the dashed arrows define a primitive unit cell of the ordered phase.

 © 1992 The American Physical Society

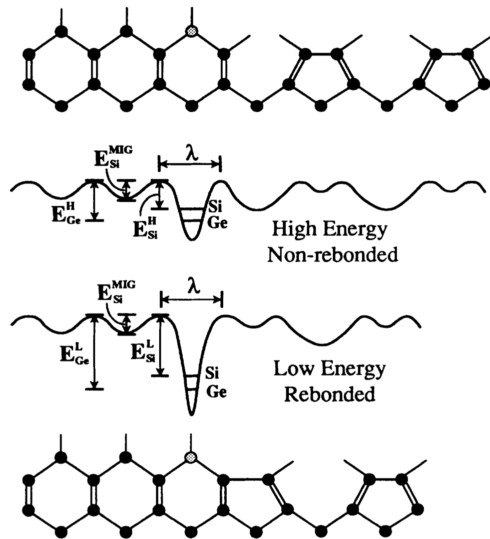

FIG. 2. [110] projection of high-energy nonrebonded and low-energy rebonded type-S_B steps with accompanying energy-level schematics (see text).

more likely to be incorporated into the new surface layer upon dimerization with a second atom in the well, as shown in Fig. 2. The two step configurations will therefore compete with each other for the available Ge flux on the surface, which in our model for alloy ordering is the key controlling factor.

Let us assume that the S_B steps advance by one dimer unit of length λ in time τ so that the island growth velocity $u=\lambda/\tau$. We treat the two species independently, so that after time τ the composition in the well will be frozen by the next monolayer of lateral growth. The relevant rate equation for the Si concentration C_{Si}^{L} present at the low-energy step at time t is then given by the difference between the arrival and desorptive flux ($\tau > t > 0$):

$$\lambda^2 \frac{\partial C_{\text{Si}}^{L}}{\partial t}(t) = D_0^{\text{Si}}[C_{\text{Si}}^{V}(t)\exp(-E_{\text{Si}}^{\text{mig}}/kT) - C_{\text{Si}}^{L}(t)\exp(-E_{\text{Si}}^{L}/kT)]\,, \quad (1)$$

where the Si preexponential factor D_0^{Si} is assumed the same for absorptive and desorptive processes. $C_{\text{Si}}^{V}(t)$ is the 2D Si "vapor" concentration, $E_{\text{Si}}^{\text{mig}}$ is the activation energy for surface diffusion, and E_{Si}^{L} is the low-energy step desorption energy (see Fig. 2). A corresponding equation exists for C_{Ge}^{L} at the same low-energy step. To solve Eq. (1), we now make the reservoir approximation $C_{\text{Si}}^{V}(t)=C_{\text{Si}}^{V}(x^V)$. This implies that in the locality of a step, the Si composition x^V in the 2D vapor remains constant over a time large compared with τ. Physically, this is justified since during time τ the diffusion lengths of Si and Ge atoms in the fast direction are of the order of 200 nm at 350 °C [15] which is considerably greater than the average distance between islands (~5 nm) [12]. Desorbed atoms will therefore explore many islands via an anisotropically shaped reservoir. Solving Eq. (1) and the corresponding equation for C_{Ge}^{L} at the low-energy step gives the concentration ratio at time τ as

$$C_{\text{Si}}^{L}/C_{\text{Ge}}^{L} = [C_{\text{Si}}^{V}(x^V)/C_{\text{Ge}}^{V}(x^V)]R^L(u,T)\,. \quad (2)$$

The factor

$$R^L(u,T) = \frac{e^{\Delta E_{\text{Si}}^{L}/kT} + [1-e^{\Delta E_{\text{Si}}^{L}/kT}]e^{-D_{\text{Si}}^{L}/u\lambda}}{e^{\Delta E_{\text{Ge}}^{L}/kT} + [1-e^{\Delta E_{\text{Ge}}^{L}/kT}]e^{-D_{\text{Ge}}^{L}/u\lambda}} \quad (3)$$

is expressed in terms of desorption energies ($\Delta E_{\text{Si}}^{L} = E_{\text{Si}}^{L} - E_{\text{Si}}^{\text{mig}}$) and the low-energy step diffusivities D_{Si}^{L} and D_{Ge}^{L}, where $D_{\text{Si}}^{L} = D_0^{\text{Si}}\exp(-E_{\text{Si}}^{L}/kT)$ [16]. $R^L(u,T)$ is a measure of the nonequilibrium segregation at the low-energy step. For high growth rates, $u \gg D_{\text{Si}}^{L}/\lambda, D_{\text{Ge}}^{L}/\lambda$ and $R^L(u,T)=1$. Then the low-energy step acts as a perfect atom trap, and the step concentration reflects the reservoir composition. Conversely, for low growth rates, we have $R^L(u,T)=\exp[(\Delta E_{\text{Si}}^{L} - \Delta E_{\text{Ge}}^{L})/kT]$ and equilibrium segregation results.

As growth proceeds alternately through high- and low-energy S_B steps, the reservoir will rapidly attain a steady-state composition. The average step composition will then equal the composition of the deposited alloy x so that at steady state

$$x^L + x^H = 2x\,, \quad (4)$$

where $\text{Si}_{x^L}\text{Ge}_{1-x^L}$ and $\text{Si}_{x^H}\text{Ge}_{1-x^H}$ represent the low- and high-energy step alloy compositions. Combining this result with the concentration ratios [Eq. (2)] for the low- and high-energy steps gives

$$x^{L^2}\left[1-\frac{R^L}{R^H}\right] + x^L\left[\frac{R^L}{R^H} + 2x\frac{R^L}{R^H} - 2x + 1\right] - 2x\frac{R^L}{R^H} = 0. \quad (5)$$

The positive root of this quadratic equation then yields the Si composition x^L [and hence x^H from Eq. (4)] as a function of R^L/R^H and the deposited alloy composition x.

We now estimate the temperature dependence of the ordering as follows. First, the appropriate activation energy and prefactor for surface diffusion in Eq. (1) should reflect the rate-determining step governing island growth [17]. For Si, these quantities have been measured [15] as $E_{\text{Si}}^{\text{mig}} = 0.67$ eV/atom and $D_0^{\text{Si}} \sim 10^{-3}\ \text{cm}^2\text{s}^{-1}$ which is in excellent agreement with recent theoretical work [18,19]. Similar measurements for Ge are presently unavailable so we assume an identical migration energy and prefactor to the Si case. However, our calculations indicate that if $E_{\text{Ge}}^{\text{mig}} > E_{\text{Si}}^{\text{mig}}$, the order parameter will increase.

The energy levels in Fig. 2 are estimated as follows. The difference between rebonded and nonrebonded steps is about 0.2 eV/atom [13] and, as discussed earlier, the difference between the Si and Ge levels is 0.1 eV/atom. Although our model is rather sensitive to the low- and high-energy step diffusivities, the relevant edge desorption energies are currently unknown. However, by treating

the Si atom desorption energy as a free parameter, we find that a best fit to the experimentally observed temperature dependence of the ordering [20] occurs for $\Delta E^L_{\rm Si} = 0.8 \pm 0.1$ eV/atom [21]. This value refers to a single atom desorbing away from the step edge and is consistent with a recent minimum value estimate for the more energetically unfavorable case of edge desorption away from a completed dimer unit [22]. This implies $\Delta E^L_{\rm Ge} = 0.9$ eV, $\Delta E^H_{\rm Si} = 0.6$ eV, and $\Delta E^H_{\rm Ge} = 0.7$ eV. Finally, for an average island separation of, say, 5 nm [12] and a 0.24-nm s^{-1} deposition rate, we estimate the mean step velocity to be 4.5 nms^{-1} [23].

Using the above estimates for the relevant parameters, the computed values of x^L and x^H for a $Si_{0.5}Ge_{0.5}$ alloy are displayed in Fig. 3. Clearly, a peak exists in the ordering at around 400 °C, but a disordered alloy is predicted at high and low temperatures. Our model can therefore reproduce the experimentally observed temperature dependence of the ordering [20] and provides a new physical explanation for ordering in semiconductor systems. At low growth temperatures, both steps in Fig. 2 act as perfect atom traps ($R^L = R^H = 1$). The atom flux arriving at the edge of an island will, therefore, be randomly frozen at the composition of the deposited alloy. At very high growth temperatures, the adatom thermal energy becomes significant compared with the depth of the potential wells, resulting in equilibrium segregation. Since both steps compete equally for Ge atoms in the reservoir, this will again produce a disordered alloy. However, at intermediate temperatures, the high-energy step will tend towards its equilibrium configuration and become Ge rich, whereas the low-energy step will still act as an effective atom trap. Ordering is, therefore, essentially a kinetic effect which peaks in a fairly narrow temperature window.

As revealed by the dashed line in Fig. 3, increasing the deposition rate forces the type-S_B steps to grow faster and shifts the ordering peak to a higher temperature by extending the kinetically frozen regime. This effect, combined with the likely sensitivity of the Si and Ge energy levels in the potential wells to substrate strain, may explain why ordering is sometimes found to occur [1,4] and is sometimes absent [20,24] from strained alloy layers grown at identical temperatures.

We now explain how phase locking can occur during monolayer island growth conditions. Starting with the ordered monolayer resulting from lateral segregation during growth [Fig. 4(a)], the next monolayer will grow along [110]. Lateral segregation will again occur although the Si and Ge atoms will now project as alloy columns [Fig. 4(b)]. Note that the translational phase of the surface dimerization is at this stage a statistical process depending on the initial nucleation of the island. For example, when two atoms dimerize, this will lock the phase of subsequent dimer bonds as further atoms bond to the island. The next monolayer of growth will then produce the ordered (2×2) surface [Fig. 4(c)]. Note that the nature of the ordering is independent of the direction of step propagation. This is an important difference between the growth of alloys and ultrathin $(Si_mGe_n)_p$ superlattices by sequential deposition. In the case of superlattice growth, the existence of several interfacial phase variants could be attributed to a Ge atom pump mechanism [7], the precise nature of the variant depending critically on the direction of step growth. This explains why, in the case of alloys, only a single phase is present. The next monolayer of growth [Fig. 4(d)] is a repeat of stage 4(b), although the two possible translational phases of the dimerization are no longer equally probable. Subsurface strain set up by the ordered monolayers will influence the dimerization direction in the initial stages of island nucleation resulting in the preferred direction shown.

Repeating the growth mechanism outlined in Fig. 4 generates the new long-range ordered phase shown in Figs. 1(c) and 1(d). Image simulation indicates that the two phases previously proposed to explain ordering in the Si-Ge system [1,2] would lead to either a clearly distinguishable pattern or much higher contrast than is observed experimentally [3]. The primitive cell in Fig. 1(c),

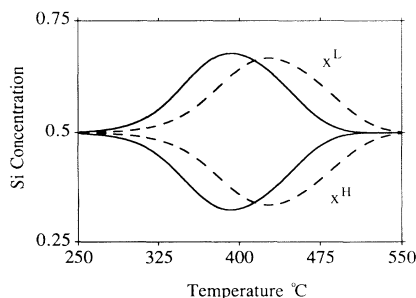

FIG. 3. Si concentration at low-energy (upper curves) and high-energy (lower curves) S_B steps as a function of substrate temperature for a $Si_{0.5}Ge_{0.5}$ deposited alloy. The solid and dashed lines correspond to deposition rates of 0.24 and 0.8 nms^{-1}, respectively.

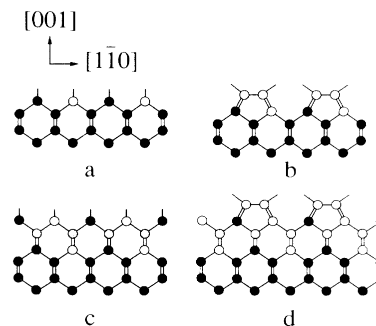

FIG. 4. Phase-locking mechanism for ordered Si-Ge growth by monolayer height islands. The growth direction is [001], and the structures are projected along [110]. Open circles represent Ge-rich columns, solid circles represent Si-rich columns, and shaded circles correspond to the deposited alloy composition.

however, produces rather weak contrast between Si-rich and Ge-rich {111} planes due to the presence of alloy columns [Fig. 1(d)] which leads to excellent agreement between simulation and experiment [Figs. 1(a) and 1(b)]. This defines ordering along two ⟨111⟩ directions so that two sets of $\frac{1}{2}$ {111} superlattice spots arise from each of the four orientational variants [25]. {110}- and {100}-type reflections remain kinematically forbidden so that the structure is totally consistent with all previous diffraction data [1,2].

The structure of the ordered phase and the transient behavior during alloy growth has several important implications. First, a "chemical surfactant" such as As, which preserves a (2×1) reconstruction on Si(001), will form deep energy levels at both steps in Fig. 2 [26]. In principle, it should therefore be possible to chemically tune the surface energetics and grow random alloys without destroying the (2×1) reconstruction. Furthermore, the recent observation of enhanced photoluminescence in MBE grown alloys [27] could be related to the details of the ordered microstructure. Understanding this link may therefore provide an exciting future prospect for Si-Ge-based optoelectronic devices.

This research was sponsored by the Division of Materials Sciences, U.S. Department of Energy, under Contract No. DE-AC05-84OR21400 with Martin Marietta Energy Systems, Inc.

[1] A. Ourmazd and J. C. Bean, Phys. Rev. Lett. **55**, 765 (1985).

[2] F. K. LeGoues, V. P. Kesan, and S. S. Iyer, Phys. Rev. Lett. **64**, 40 (1990).

[3] D. E. Jesson, S. J. Pennycook, and J.-M. Baribeau, in *High-Resolution Electron Microscopy of Defects in Materials*, edited by R. Sinclair, D. J. Smith, and U. Dahmen, MRS Symposia Proceedings No. 183 (Materials Research Society, Pittsburgh, 1990).

[4] D. J. Lockwood *et al.*, Solid State Commun. **61**, 465 (1987).

[5] F. K. LeGoues *et al.*, Phys. Rev. Lett. **64**, 2038 (1990).

[6] S. de Gironcoli, P. Giannozzi, and S. Baroni, Phys. Rev. Lett. **66**, 2116 (1991).

[7] D. E. Jesson, S. J. Pennycook, and J.-M. Baribeau, Phys. Rev. Lett. **66**, 750 (1991).

[8] S. J. Pennycook and D. E. Jesson, Phys. Rev. Lett. **64**, 938 (1990).

[9] The alloy layer was 350 nm thick and relaxed. Further growth details are provided in J.-M. Baribeau *et al.*, J. Appl. Phys. **63**, 5738 (1988).

[10] Although clearly appreciating the link with the (2×1) surface, the growth model proposed in Ref. [5] requires bilayer step flow and significant subsurface diffusion. The authors of Ref. [11] have shown for Si homoepitaxy that bilayer step flow takes place in a narrow temperature window around 540 °C. At 350 °C, growth occurs by monolayer height islands. It is unlikely that this temperature dependence could be shifted by 200 °C during alloy deposition.

[11] A. J. Hoeven *et al.*, Thin Solid Films **183**, 263 (1989).

[12] R. J. Hamers, U. K. Köhler, and J. E. Demuth, J. Vac. Sci. Technol. A **8**, 195 (1990).

[13] D. J. Chadi, Phys. Rev. Lett. **59**, 1691 (1987).

[14] P. C. Kelires and J. Tersoff, Phys. Rev. Lett. **63**, 1164 (1989).

[15] Y. W. Mo, J. Kleiner, M. B. Webb, and M. G. Lagally, Phys. Rev. Lett. **66**, 1998 (1991).

[16] Similar expressions are familiar in the fields of rapid solidification or laser annealing; see, for example, M. J. Aziz, J. Appl. Phys. **53**, 1158 (1982); W. Kurz and D. J. Fisher, *Fundamentals of Solidification* (Trans Tech, Switzerland, 1989).

[17] x^L is insensitive to the absolute value of this quantity, somewhat justifying the neglect of anisotropic diffusion in Eq. (1).

[18] G. Brocks, P. J. Kelly, and R. Car, Phys. Rev. Lett. **66**, 1729 (1991).

[19] D. Srivastava and B. J. Garrison, J. Chem. Phys. **95**, 6885 (1991).

[20] F. K. LeGoues, V. P. Kesan, T. S. Kuan, and S. S. Iyer, in Proceedings of the First Topical Symposium on Si Based Heterostructure, Toronto, 1990 (unpublished), p. 100.

[21] Changing the relative energy levels in Fig. 2 by ±0.1 eV/atom primarily influences the magnitude of the order parameter. The peak position in Fig. 3 is sensitive to the absolute well depth and is displaced by ±50 °C for a ±0.1-eV/atom shift in the desorption energies.

[22] M. G. Lagally *et al.*, in *Kinetics of Ordering and Growth at Surfaces*, edited by M. G. Lagally (Plenum, New York, 1990), p. 145.

[23] It was shown in Ref. [15] that for low supersaturations and coverages, the mean island separation is weakly dependent on the surface diffusion coefficient. The step velocity will therefore change by a factor of only 2 between 250 and 550 °C which does not appreciably influence the ordering kinetics. This situation must be qualitatively similar at higher supersaturations, justifying a temperature-independent step velocity.

[24] T. S. Kuan, S. S. Iyer, and E. M. Yeo, in *Proceedings of the Forty-Seventh Annual Meeting EMSA* (San Francisco Press, San Francisco, 1989), p. 580.

[25] A total of eight possible variants can exist of which only four can be grown.

[26] As estimated by M. Copel, M. C. Reuter, M. Horn von Hoegen, and R. M. Tromp, Phys. Rev. B **42**, 11 682 (1990), the As levels will be approximately 0.1 eV/atom lower than the Ge levels.

[27] J-P. Noël, N. L. Rowell, D. C. Houghton, and D. D. Perovic, Appl. Phys. Lett. **57**, 1037 (1990).

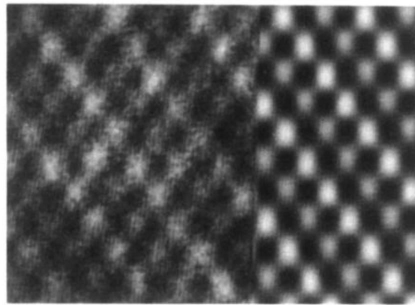

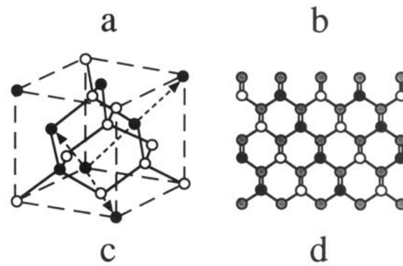

FIG. 1. (a) [110] Z-contrast image of an ordered $Si_{0.6}Ge_{0.4}$ alloy deposited at 0.24 $nm\,s^{-1}$ on a Si(001) substrate at $350 \pm 25\,°C$ [9]. The accompanying simulation (b) is generated from the [110] projection (d) of the ordered phase (c) predicted by our lateral segregation model. Each bright spot in the image corresponds to a [110] atomic dumbbell, and the column intensities approach the atomic-number-squared dependence of unscreened Rutherford scattering. The open, solid, and shaded circles represent Ge-rich, Si-rich, and deposited alloy compositions, respectively. In (c) the dashed arrows define a primitive unit cell of the ordered phase.

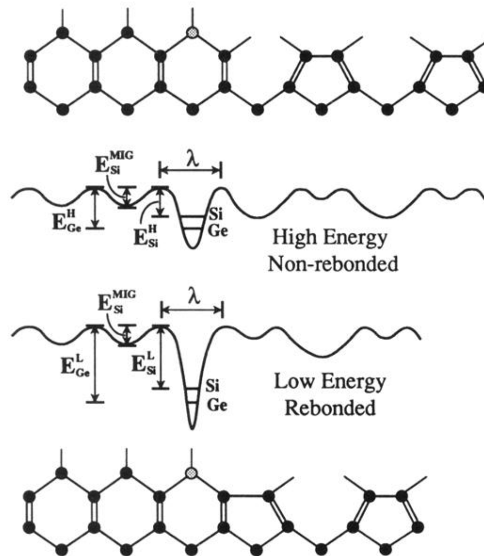

FIG. 2. [110] projection of high-energy nonrebonded and low-energy rebonded type-S_B steps with accompanying energy-level schematics (see text).

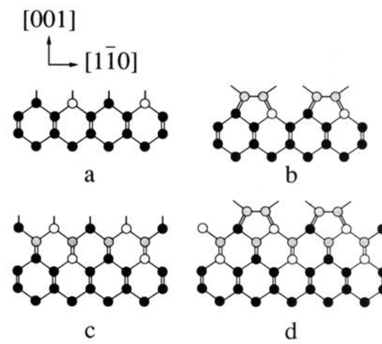

FIG. 4. Phase-locking mechanism for ordered Si-Ge growth by monolayer height islands. The growth direction is [001], and the structures are projected along [110]. Open circles represent Ge-rich columns, solid circles represent Si-rich columns, and shaded circles correspond to the deposited alloy composition.